J Mater Sci (2007) 42:2086–2089
DOI 10.1007/s10853-006-1210-5

Preparation and microwave absorption properties of nanosized Ni/$SrFe_{12}O_{19}$ magnetic powder

Xifeng Pan · Jianxun Qiu · Mingyuan Gu

Received: 17 November 2005 / Accepted: 30 January 2006 / Published online: 9 December 2006

Abstract A new type of Ni-coated strontium ferrite powder was prepared with electroless plating enhanced by ultrasonic wave at room temperature. The morphology, crystal structure and microwave absorption properties of the Ni-coated powder were investigated with field emission scanning electron microscopy (FE-SEM), X-ray diffraction (XRD), EDS and vector network analyzer. The results show that the powder possesses excellent microwave absorption properties. The maximum microwave loss of the composite powder reaches –41.3 dB. The bandwidth with the loss above –10 dB reaches 8 GHz.

Introduction

Eletromagnetic wave absorbers are becoming more and more important for our society. They are widely used in microwave devices and electromagnetic shielding field [1, 2]. Recent studies [3, 4] indicate that the hexagonal strontium ferrite is a kind of good microwave absorber. It is more adapted to be used in high frequency band than the ferrites with spinel and garnet structure. But, the susceptibility of ferrites is low, which makes it difficult to further improve their microwave absorption property. The susceptibility of metal powder is high [5, 6]. But, as microwave absorber, it is often confined by the skin effect. Obviously, the best way to solve these problems is fabricating the composite of ferrite and metal powder efficiently. However, very few works have been done on it to this day. In this paper, a new type of nanosized Ni/$SrFe_{12}O_{19}$ powder was fabricated with electroless plating enhanced by ultrasonic wave at room temperature for the first time. The powder is expected to possess the advantages of both ferrite and metal powder. The microwave absorption properties of the powder were studied.

X. Pan (✉) · M. Gu
State Key Laboratory of MMCs, Shanghai Jiaotong University, 1954 Huashan Road, Shanghai 200030, China
e-mail: xifengpan@sjtu.edu.cn

J. Qiu
School of Environmental and Materials Engineering, Yantai University, Yantai 264005, China

Experimental

The strontium ferrite powder was prepared first. According to the composition of $SrFe_{12}O_{19}$, stoichiometric amount of $Sr(NO_3)_2$ and $Fe(NO_3)_3{\cdot}9H_2O$ were dissolved in deionized water followed by the addition of citric acid. An ammonia solution was added to adjust the pH value to 7.0. The solution was slowly evaporated at 80 °C until a viscous gel was formed. It was dried at 110 °C and turned into a dry precursor gel. The precursor gel was ignited in air and burned into a dendritic and brittle powder. After the calcination at 850 °C for one and a half hours the $SrFe_{12}O_{19}$ nanopowder was successfully synthesized.

The strontium ferrite powder was pretreated to produce catalytic activity through the following procedures: Coarse → Rinsing → Sensitization → Activation → Rinsing and drying at 80 °C in air. After pretreatment, the strontium ferrite powder was put into the plating solution in a beaker. And then, the beaker was immersed in the water bath of a BRANSON SB2200 ultrasonic generator. The parameters in

the electroless plating process are $NiSO_4{\cdot}6H_2O$(30 g/l), $NaH_2PO_2{\cdot}H_2O$(20 g/l), $Na_3C_6H_5O_7{\cdot}2H_2O$(15 g/l), CH_2COONa (15 g/l), PH (5–6), temperature (25–35 °C), load (5–20 g/L). The phases of the plated powders were identified with X-ray diffraction (XRD) analysis. The particles' morphology was observed with field emission scanning electron microscopy **(**FE-SEM) before and after plating. The composition of the plating layer was analyzed by energy dispersive analysis of X-rays (EDS) technology.

The microwave absorption properties were expressed in microwave loss efficiency. The composite powder was filled into a 30 mm × 30 mm × 3 mm polytetrafluoroethylene box and pressed tightly. The transmission and reflection coefficients were measured with microstrip transmission line in an 8722ES vector network analyzer in the frequency range from 5 G to 15 GHz. The microwave loss A_{dB} was calculated according to Eq. 1.

$$A_{dB} = 10 \log \frac{P_T}{P_I - P_R} \quad (1)$$

where P_T is the transmission wave power; P_I is the incident wave power and P_R is the reflection wave power. The microwave loss of the polytetrafluoroethylene box was subtracted.

Results and discussion

Electroless plating process

Generally, during electroless plating, self-catalysis reduction reaction on the sample surface can be described as follows:

$$Ni^{2+} + H_2PO_2^- + H_2O \rightarrow HPO_3^{2-} + 3H^+ + Ni$$

$$H_2PO_2^- + [H] \rightarrow H_2O + OH^- + P$$

$$H_2PO_2^- + H_2O \rightarrow H[HPO_3]^- + H_2$$

The reaction process needs to absorb outside energy. Heating to 65–95 °C is required for the electroless plating of the powder in micron scale [7, 8]. But, the nanoparticle has higher surface energy, and after stimulation by ultrasonic wave, deposition on its surface spontaneously occurs at room temperature (25–35 °C) [9]. For nickel-plating experiment in this paper, deposition occurred about 20 min later with H_2 bubbles evaporating out of the solution. During the plating process, the solution remained transparent, and the self-dissolution and precipitation didn't appear. The color of the as-plated powders changed from brown to black with the load changing from 20 g/L to 5 g/L.

Crystalline structure and morphology analyses of the powders

FE-SEM images of the strontium ferrite powder and the as-plated powder (load = 5.0 g/L) are shown in Fig. 1. It can be seen that the strontium ferrite powder is successfully coated with Ni–P alloy. Some particles are seamed together by the deposited layer. The surface of the as-plated powder looks very rough. This is likely to be related to the gas release kinetics involved in the plating process. Accompanying with the reduction of nickel, hydrogen gas is released during the plating, and in turn, will disturb the formation and deposition of nickel particles on the surface of the strontium ferrite powder. Clearly, the ultrasonic wave leads to a rapid release of the hydrogen gas. As a result, the metal grains will grow outwards along the paths of the released gas, forming plate-like and needle-shaped particles. Naturally, the surface of the deposited layer will become very rough and porous. The average size for the strontium ferrite powder is estimated in Fig. 1. It is respectively about 95 nm and 110 nm. So, the average coating thickness is evaluated as about 8 nm.

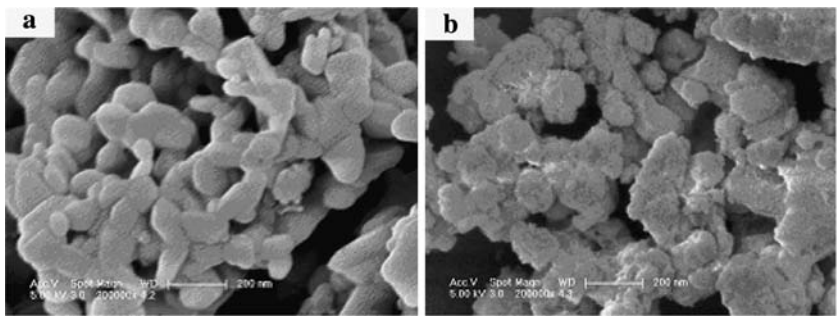

Fig. 1 FE-SEM images for (**a**) the strontium ferrite powder; (**b**) the as-plated powder

The XRD spectra of the as-plated powder and the plated powder after heat treatment at 400 °C for 1 h in N_2 flow are shown in Fig. 2. It can be seen that the as-plated layer on the surface of the strontium ferrite powder is noncrystalline. The Ni–P can't be detected. After heat treatment, the Ni_3P sharp diffraction peaks appear and the plated layer crystallizes. There are also several unknown peaks on the XRD spectra. They are supposed to be the impurities, which were induced during the plating process. Further study is also needed to optimize the plating process. The plated powder was also detected by EDS to determine the composition of the deposition layer. Ni, P, Sr and Fe elements were all found. So, we believe that the powder is the composite of $SrFe_{12}O_{19}$ and Ni–P. The EDS results also show that the average content of phosphorus in the plated layer is about 16.74 wt%.

Microwave absorption properties of the powders

The microwave transmission losses of the powders are displayed in Fig. 3(a–e). The load of all the plated samples in Fig. 3 is 10 g/L. As it is shown in Fig. 3, the microwave losses of the strontium ferrite powder are increased by the plating of Ni–P deposited layer. And the frequency bandwidth with the loss above –10 dB is broadened greatly. From Fig. 3(b), it can be seen that the noncrystalline deposited layer will increase the microwave absorption properties also. This result indicates that the noncrystalline paramagnetic deposited layer changed the surface condition of the strontium ferrite powder, which made it easier for the microwave to penetrate into the core strontium ferrite powder and be absorbed. The maximum absorption peak (–41.3 dB at 9.2 GHz) and the widest bandwidth (about 8 GHz) appears in Fig. 3(c). The Ni–P deposited layer on the surface of inner strontium ferrite powder crystallizes when the heat treatment temperature reaches 400 °C. And the magnetism of the deposited layer is improved greatly. Then the interaction at the interface of the deposited layer and the strontium ferrite powder becomes strong. The interface polarization and multiple scatter increase the microwave absorption [10]. Studies [11–13] show that the surface spins of ferrite nanoparticles are disordered, and the exchange-coupling interaction at the interface of two magnetic phases occurs. The surface spin can result in a high magnetic loss. Then, the microwave absorption is improved. It is deduced from Fig. 3(d, e) that the microwave absorption decreases with the enhancement of heat treatment temperature, which maybe resulted from the increasing of the grain size in the plated layer. It is also can be seen that the frequency of the loss peak decreases gradually with the increasing of the heat treatment temperature. The work of Herzer [14] shows the exchange-coupling interaction will decrease the magnetocrystalline anisotropy field (H_a) of the magnetic materials. The ferromagnetic resonant frequency of the strontium ferrite with uniaxial anisotropy is

$$f = \frac{\gamma}{2\pi} H_a \tag{2}$$

where γ is the gyromagnetic ratio. With the decreasing of the H_a, the ferromagnetic resonant frequency decreases also.

The effects of the load on the microwave absorption properties of the composite powder were studied also.

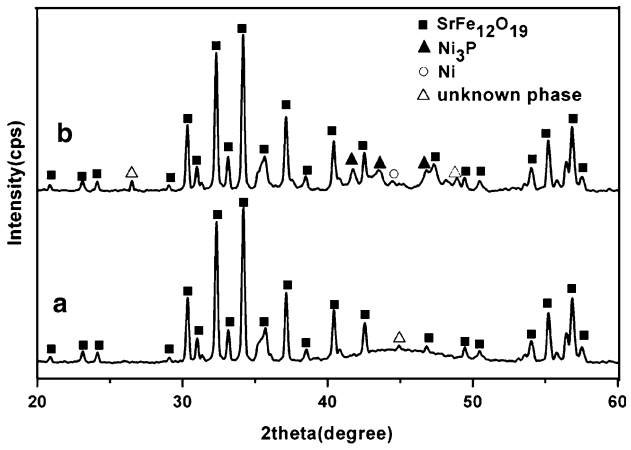

Fig. 2 XRD spectra for (**a**) the as-plated powder; (**b**) the plated powder after heat treatment at 400 °C for 1 h in N_2 flow

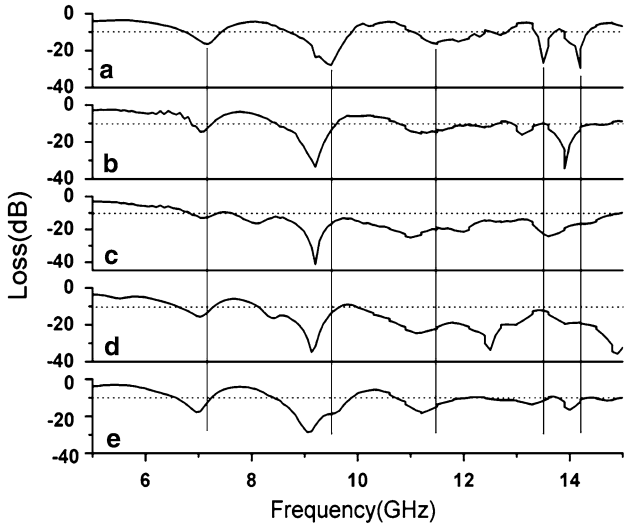

Fig. 3 Microwave loss spectra for (**a**) the strontium ferrite powder; (**b**) the as-plated powder; (**c**)–(**e**) the plated powder after heat treatment at 400 °C, 500 °C, 600 °C for 1 h in N_2 flow

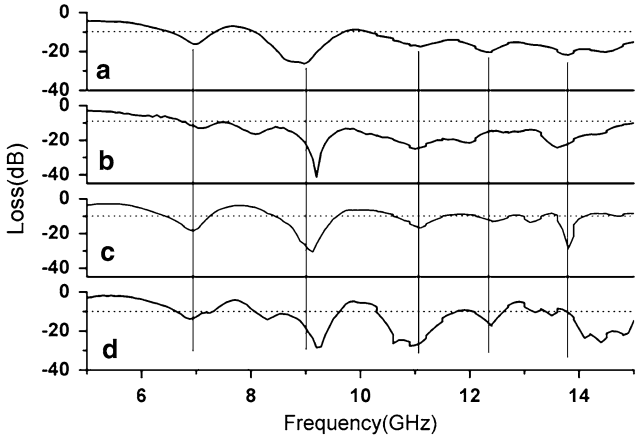

Fig. 4 Microwave loss spectra for the powders (**a**) load = 5 g/L; (**b**) load = 10 g/L; (**c**) load = 15 g/L; (**d**) load = 20 g/L

All the plated powders were heattreated at 400 °C for 1 h in N_2 flow. Fig. 4 shows the microwave loss spectra of the plated powders with different loads.

As shown in Fig. 4, the microwave absorption of the powders doesn't increase with the decreasing of the load. There is a best load, and it is 10 g/L. With the increasing of load, the frequency of the second loss peak moves towards high frequency gradually. Because the deposited layer becomes thinner with the increasing of the load, the weight ratio of the strontium ferrite in the composite powder increases. And, the strontium ferrite possesses a higher magnetocrystalline anisotropy field. Therefore, the loss peak moves to high frequency.

Conclusions

An electroless plating technology enhanced with ultrasonic wave was successfully employed in fabricating a new kind of Ni-coated strontium ferrite magnetic powder. The as-plated layer on the surface of the strontium ferrite particle was a noncrystalline Ni–P alloy. After heat treatment at 400 °C for 1 h in the N_2 flow, the deposition layer was crystallized obviously and a Ni_3P phase can also be detected. The plated powders possess more effective microwave absorption properties than the conventional strontium ferrite powder. The maximum microwave loss of the plated powders reaches –41.3 dB. The bandwidth with the loss above –10 dB reaches 8 GHz.

Acknowledgements The authors are grateful to the Instrumental Analysis Centre of the Shanghai Jiao Tong University for providing the XRD, EDS and FE-SEM analyses.

References

1. Dishovske N, Petkov A, Nedkov Iv (1994) IEEE Trans Magn 30:969
2. Dou YW (1996) Ferrite. Jiangsu Science and Technology Press, Nanjing
3. Verma A, Mendiratta RG, Goel TC, Dube DC (2002) J Electroceram 8:203
4. Fang QQ, Liu YM, Li XG (2001) J Magn Magn Mater 234:366
5. Ding J, shi Y, Chen LF, Deng CR, Fuh SH, Li Y (2002) J Magn Magn Mater 247:249
6. Zhou PH, Xie LJ, lang DF, Chen L, Zhao XQ (2005) J Magn Magn Mater 292:325
7. Ramaseshan R, Seshadri SK, Nair NG (2001) Scripta Materialia 45:183
8. Wen G, Guo ZX, Davies CKL (2000) Scripta Materialia 43:307
9. Ling GP, Li Y (2005) Mater Lett 59:1610
10. Liu B, Guan JG, Wang Q, Zhang QJ (2005) J Funct Mater Cont 36:133. (in chinese)
11. Gazeau F, Dubois E, Hennion M et al (1997) Europhys Lett 40:575
12. Guan JG, Wang W, Gong RZ et al (2002) Langmuir 18:4189
13. Kodama RH, Berkowitz AE (1999) Phys Rev B 59:6321
14. Herzer G (1990) IEEE Trans Magn 26:1397